 Bull. Chem. Soc. Jpn. Vol. 79, No. 10, 1525–1534 (2006)

Syntheses and Crystal Structures of Mono(2,2′-bipyridine)dichlorobis-(dimethyl sulfoxide-*S*)ruthenium(II) Complexes, [$RuCl_2$(bpy)(dmso-*S*)$_2$]

Mari Toyama,* Ken-ichi Inoue, Shinobu Iwamatsu, and Noriharu Nagao*

Department of Applied Chemistry, Meiji University, Kawasaki 214-8571

Received January 23, 2006; E-mail: nori@isc.meiji.ac.jp

The reaction between *trans*-[$RuCl_2$(dmso-*S*)$_4$] (dmso = dimethyl sulfoxide) and 2,2′-bipyridine (bpy) in EtOH–H_2O afforded *trans*(Cl),*cis*(S)-[$RuCl_2$(bpy)(dmso-*S*)$_2$] (**1**) in good yield. When dissolved in DMSO, **1** rearranged to the thermodynamically more stable *cis*(Cl),*cis*(S)-[$RuCl_2$(bpy)(dmso-*S*)$_2$] (**2**) along with a small amount of *cis*(Cl),-*trans*(S)-[$RuCl_2$(bpy)(dmso-*S*)$_2$] (**3**). Isomer **2** was selectively synthesized by heating **1** in EtOH–DMSO (9:1) and, more conveniently, by the reaction of *cis*(Cl),*fac*(S)-[$RuCl_2$(dmso-*S*)$_3$(dmso-*O*)] with bpy in EtOH–DMSO (9:1). The structures of **1**, **2**, and **3** were determined using single-crystal X-ray crystallography. The crystal structure of **1** revealed that the 6- and 6′-protons of the bpy ligand repulsed the two dmso ligands within the equatorial plane, resulting in the lower thermodynamic stability of **1**. In contrast, the crystal structure of **2** showed that its bpy ligand is involved in hydrogen bonding with the monodentate dmso and Cl^- ligands within the equatorial plane. Our studies show that hydrogen bonds within the equatorial plane of **2** restrict the conformation of the dmso ligands in the crystal and in DMSO.

Ruthenium polypyridyl complexes have been extensively investigated for their photochemical and electrochemical properties.[1–4] Due to their synthetic availability, most of the ruthenium polypyridyl complexes that have been evaluated are homoleptic or bis-heteroleptic polypyridyl complexes. To date, only a few synthetic routes for tris-heteroleptic polypyridyl complexes have been reported,[5–14] because it is difficult to synthesize the precursor, i.e., the mono(polypyridyl)ruthenium complex. Evans and co-workers have reported the syntheses of mono(polypyridyl)ruthenium complexes by refluxing *cis*(Cl),-*fac*(S)-[$RuCl_2$(dmso-*S*)$_3$(dmso-*O*)] (dmso = dimethyl sulfoxide) and a polypyridyl ligand in chloroform.[5] Although this method has been utilized to prepare mono(polypyridyl)ruthenium complexes, [$RuCl_2$(bpy)(dmso-*S*)$_2$] (bpy = 2,2′-bipyridine) is obtained as a mixture of geometrical and linkage isomers, in which their structures have yet to be elucidated.[7] However, when an unsymmetrical *N*,*N*′-chelating ligands (L), instead of bpy, was used in the reaction with *cis*(Cl),-*fac*(S)-[$RuCl_2$(dmso-*S*)$_3$(dmso-*O*)] in MeOH, *trans*(Cl),*cis*(S)-[$RuCl_2$(L)(dmso-*S*)$_2$] was obtained.[15,16] Sens and co-workers have synthesized and characterized two isomers of the ruthenium dimethyl sulfoxide complexes that contain 3,5-bis(2-pyridyl)pyrazole (Hbpp), *trans*(Cl),*cis*(S)- and *cis*(Cl),*cis*(S)-[$RuCl_2$(Hbpp)(dmso-*S*)$_2$].[16]

In the case of our mono(2,2′-bipyridine)ruthenium complex, *trans*-[$RuCl_2$(dmso-S_4)], which was synthesized and characterized by Alessio and co-workers,[17] was used as the starting material, rather than the conventional *cis*-isomer. In aqueous solutions, the *trans*-isomer immediately released two dmso ligands to form *trans*(Cl),*cis*(O)-[$RuCl_2(OH_2)_2$(dmso-*S*)$_2$], which has two labile sites at the *cis*-position that are suitable for accepting an incoming bipyridine ligand. Furthermore, for this *cis*-diaqua species, the two Cl^- ligands, which are *trans* to each other and less labile, protect the species from subsequent attacks by other bipyridine ligands. Because it is well known that *trans*-[$RuCl_2$(dmso-*S*)$_4$] possesses significant antitumor and antimetastatic activity,[17–19] the complex should be reactive towards proligands at ambient temperatures. Therefore, the preparation of a mono(2,2′-bipyridine)ruthenium complex presumably involves the reaction of *trans*-[$RuCl_2$-(dmso-*S*)$_4$] with bpy in aqueous EtOH at low temperatures.

In this paper, convenient syntheses and crystal structures of two isomers of the mono(2,2′-bipyridine)ruthenium complex *trans*(Cl),*cis*(S)-[$RuCl_2$(bpy)(dmso-*S*)$_2$] (**1**) and *cis*(Cl),*cis*(S)-[$RuCl_2$(bpy)(dmso-*S*)$_2$] (**2**) are reported. Furthermore, the crystal structure of the remaining isomer, *cis*(Cl),*trans*(S)-[$RuCl_2$(bpy)(dmso-*S*)$_2$] (**3**), is also reported.

It is well known that traditional hydrogen bonds (OH···O, NH···O, OH···N, or NH···N) play an important role in the construction and stabilization of supramolecular assemblies.[20–23] In contrast, the X-ray structure of **2** showed that the 6-proton of the bpy ligand interacts with the O atom of the dmso ligand (CH···O hydrogen bond) within the same equatorial plane. The concept of non-classical hydrogen bonding, such as CH···O interactions, has recently gained much interest.[24–31] Although weaker than classical hydrogen bonds, such non-classical hydrogen bonds have been shown to be significant in the stabilization of nucleic and protein structures.[32–34] In coordination chemistry, CH···O hydrogen bonds can be intermolecular[35,36] or intramolecular[37–40] which stabilize the crystal packing; in some cases, such bonds significantly influence the behavior of the complexes in solution. For the bis(2,2′-bipyridine)ruthenium complex with a dmso ligand, Hesek and co-workers have reported the importance of the CH···O intramolecular hydrogen bond between the sulfoxide oxygen and the hydrogen atom on the 6-position of the bpy ligand.[39,40] Furthermore, the interaction between a coordinated Cl^- ligand and a CH moiety (CH···Cl–M) has also been reported as a non-classical weak hydrogen bond and has attracted significant attention in chemical, crystallographic, and crystal engineering.[41–47] Flower and

Published on the web October 10, 2006; doi:10.1246/bcsj.79.1525

co-workers have reported hydrogen bonding between the Cl atom and 6(6′)-protons of the phenyl rings of two PPh_3 ligands in the crystal structure of *trans*(PPh_3),*cis*(Cl,CO)-[RuCl(CO)-(η^2-*C*,*N*-$C_6H_5C(H)NC_6H_4$-4Me)(PPh_3)$_2$].[42] In addition, Cini and co-workers have reported on the influence of weak intramolecular hydrogen bonding between a Cl^- ligand and the proton on the methyl group of dmso on the conformation of the dmso ligand in the crystal structure of $[PtCl_3(dmso\text{-}S)]^-$.[44] We have also observed that CH···O and CH···Cl–Ru non-bonding interactions between bpy and the dmso or Cl^- ligands significantly influence the conformation of the dmso ligands of the isomers in the crystal and in DMSO.

Experimental

Hydrated ruthenium trichloride, $RuCl_3 \cdot 3H_2O$, was purchased from Furuya Kinzoku Co. All other solvents and chemicals were of reagent quality and were used without further purification. The starting materials, *cis*(Cl),*fac*(S)-[$RuCl_2$(dmso-*S*)$_3$(dmso-*O*)] and *trans*-[$RuCl_2$(dmso-*S*)$_4$], were prepared according to the literature.[5,17] All reactions were carried out under an argon atmosphere.

Synthesis of *trans*(Cl),*cis*(S)-[$RuCl_2$(bpy)(dmso-*S*)$_2$] (1). To a solution of *trans*-[$RuCl_2$(dmso-*S*)$_4$] (2.00 g, 4 mmol) in H_2O (40 mL) was added a solution of bpy (0.64 g, 4 mmol) in EtOH (40 mL). After stirring the reaction mixture for 40 h at ca. 0 °C, the resulting red-brown precipitate, *trans*(Cl),*cis*(S)-[$RuCl_2$(bpy)(dmso-*S*)$_2$]$\cdot H_2O$ (**1**$\cdot H_2O$), which gradually appeared, was collected by filtration, washed with cold EtOH, and dried in vacuo (1.75 g, yield 87%). Red-brown crystals that were suitable for X-ray crystallography were grown over several days from the reaction mixture at ca. 0 °C without stirring. Anal. Calcd for $C_{14}H_{22}N_2Cl_2O_3S_2Ru$: C, 33.47; H, 4.41; N, 5.58%. Found: C, 33.12; H, 4.34; N, 5.46%. ^{1}H NMR (270 MHz, DMSO-d_6): δ 3.41 (12H, s, CH_3 of dmso), 7.65 (2H, dd, J = 7.5, 5.8 Hz, H-5), 8.15 (2H, t, J = 7.5 Hz, H-4), 8.62 (2H, d, J = 7.5 Hz, H-3), 9.65 (2H, br s, H-6).

Synthesis of *cis*(Cl),*cis*(S)-[$RuCl_2$(bpy)(dmso-*S*)$_2$] (2). Method A: A suspension of **1**$\cdot H_2O$ (2.00 g, 4 mmol) in a mixture of EtOH (45 mL) and DMSO (5 mL) was allowed to reflux for 1.5 h under argon. While refluxing, the suspension of red-brown solid gradually became homogeneous (after 0.5 h), followed by the gradual appearance of an orange precipitate, *cis*(Cl),*cis*(S)-[$RuCl_2$(bpy)(dmso-*S*)$_2$] (**2**). The orange precipitate was collected by filtration, washed with cold EtOH, and dried in vacuo (1.90 g, yield 95%). Orange needle crystals of **2** that were suitable for X-ray crystallography were obtained by vapor diffusion of diethyl ether into an acetonitrile solution of **2**. Anal. Calcd for $C_{14}H_{20}N_2Cl_2O_2S_2Ru$: C, 34.71; H, 4.16; N, 5.78%. Found: C, 34.72; H, 4.12; N, 5.88%. ^{1}H NMR (270 MHz, DMSO-d_6): δ 2.28 (3H, s, CH_3 of dmso), 2.98 (3H, s, CH_3 of dmso), 3.37 (3H, s, CH_3 of dmso), 3.40 (3H, s, CH_3 of dmso), 7.60 (1H, dd, J = 7.5, 5.7 Hz, H-5), 7.77 (1H, dd, J = 7.5, 5.7 Hz, H-5), 8.10 (1H, t, J = 7.5 Hz, H-4), 8.21 (1H, t, J = 7.5 Hz, H-4), 8.60 (1H, d, J = 7.5 Hz, H-3), 8.65 (1H, d, J = 7.5 Hz, H-3), 9.56 (1H, d, J = 5.7 Hz, H-6), 9.66 (1H, d, J = 5.7 Hz, H-6).

Method B: A solution of *cis*(Cl),*fac*(S)-[$RuCl_2$(dmso-*S*)$_3$-(dmso-*O*)] (2.00 g, 4 mmol) and bpy (0.64 g, 4 mmol) in EtOH (36 mL) and DMSO (4 mL) was refluxed for 1.5 h. The resulting orange precipitate, *cis*(Cl),*cis*(S)-[$RuCl_2$(bpy)(dmso-*S*)$_2$] (**2**), which gradually appeared, was collected by filtration, washed with cold EtOH, and dried in vacuo (1.70 g, yield 85%).

Isomerization of 2 to *cis*(Cl),*trans*(S)-[$RuCl_2$(bpy)(dmso-*S*)$_2$] (3). A solution of **2** in DMSO-d_6 was sealed in an NMR tube and heated to 90 °C. After 1 h, based on ^{1}H NMR spectroscopy, the isomerization of **2** afforded a mixture of **2** and **3** (85/15). To further characterize the minor product **3**, bulk sample was prepared by heating **2** (250 mg) in DMSO at 90 °C for 1 h, followed by the addition of EtOH and diethyl ether to precipitate the product. The ^{1}H NMR spectrum of the resulting bulk products were identical to that obtained from the NMR-scale reaction. Single crystals, which consisted of orange needle crystals of **2** and red block crystals of *cis*(Cl),*trans*(S)-[$RuCl_2$(bpy)(dmso-*S*)$_2$]$\cdot 0.5H_2O$ (**3**$\cdot 0.5H_2O$), were obtained by vapor diffusion of diethyl ether into an DMSO–EtOH (1:20) solution of the product. The red block crystals were mechanically separated and characterized using ^{1}H NMR spectroscopy and X-ray crystallography. For **3**, ^{1}H NMR (270 MHz, DMSO-d_6): δ 2.88 (12H, s, CH_3 of dmso), 7.65 (2H, dd, J = 8.1, 5.6 Hz, H-5), 8.07 (2H, t, J = 8.1 Hz, H-4), 8.50 (2H, d, J = 8.1 Hz, H-3), 9.39 (2H, d, J = 5.6 Hz, H-6).

X-ray Crystallography. Data for all crystals were collected using the ω-2θ scan technique ($2\theta < 55°$) on a Rigaku AFC-7R automated four-circle X-ray diffractometer equipped with a graphite-monochromatized Mo Kα radiation (λ = 0.71069 Å) at 23 °C. All calculations were carried out on an O_2 workstation (SGI) using the teXsan crystallographic software package.[48] The structures were solved by direct methods and expanded using Fourier techniques. The non-hydrogen atoms were refined anisotropically. Hydrogen atoms were placed in idealized positions and included in the structure factor calculations. For **3**, the disordered H_2O (0.5 molecules) was included at two sites: 1) special position with 0.2 occupancy, and 2) general position with 0.3 occupancy. The hydrogen atoms of the disordered solvent H_2O were not included in the structure factor calculations. The crystallographic data for **1**$\cdot H_2O$, **2**, and **3**$\cdot 0.5H_2O$ are summarized in Table 1.

Crystallographic data have been deposited with Cambridge Crystallographic Data Centre: Deposition numbers CCDC-608685–608687 for compound Nos. **1**, **2**, and **3**, respectively. Copies of the data can be obtained free of charge via http://www.ccdc.cam.ac.uk/conts/retrieving.html (or from the Cambridge Crystallographic Data Centre, 12, Union Road, Cambridge, CB2 1EZ, UK; Fax: +44 1223 336033; e-mail: deposit@ccdc.cam.ac.uk).

Results and Discussion

Synthesis and Structure of *trans*(Cl),*cis*(S)-[$RuCl_2$(bpy)-(dmso-*S*)$_2$]$\cdot H_2O$ (1$\cdot H_2O$). The reaction of bpy ligand with *trans*-[$RuCl_2$(dmso-*S*)$_4$] at 0 °C afforded only **1** in a high yield (≈90%), and spontaneous precipitation allowed for convenient collection without further purification. The ^{1}H NMR spectrum of **1** in DMSO-d_6 is shown in Fig. 1, and only four signals with intensities of 2H in the aromatic region and a singlet with an intensity of 12H in the aliphatic region were observed. The intensities of the signals indicate that **1** possesses one bpy and two dmso ligands. The spectral pattern indicates that the two pyridine rings of the bpy ligand are equivalent, in other words, two identical ligands occupy the *trans*-positions to the bpy ligand. The ^{1}H NMR spectrum suggests that the two dmso ligands of *trans*-[$RuCl_2$(dmso-*S*)$_4$] were substituted by a bpy ligand to afford the mono(2,2′-bipyridine)ruthenium complex *trans*(Cl),*cis*(S)-[$RuCl_2$(bpy)(dmso-*S*)$_2$] in which the *trans*(Cl)-configuration of the starting material was retained.

The reaction mixture was allowed to stand at ca. 0 °C without stirring for several days, which resulted in the formation of

Table 1. Crystallographic Data for **1**, **2**, and **3**

	1·H_2O	**2**	**3**·0.5H_2O
Empirical formula	$RuC_{14}N_2O_3S_2Cl_2H_{22}$	$RuC_{14}N_2O_2S_2Cl_2H_{20}$	$RuC_{14}N_2O_{2.50}S_2Cl_2H_{21}$
Formula weight	502.44	484.42	493.43
Crystal system	orthorhombic	triclinic	triclinic
Space group	*Pccn* (# 56)	$P\bar{1}$ (# 2)	$P\bar{1}$ (# 2)
Lattice parameters			
a/Å	13.948(3)	12.817(2)	9.334(3)
b/Å	19.257(4)	14.195(2)	15.611(5)
c/Å	14.092(5)	12.649(2)	7.820(2)
α/°	90	111.17(1)	97.43(2)
β/°	90	117.86(1)	105.61(2)
γ/°	90	90.15(1)	103.52(2)
V/Å^3	3785(2)	1855.9(6)	1044.3(5)
Z	8	4	2
D_{calcd} (g cm^{-1})	1.763	1.734	1.569
F_{000}	2032.00	976.00	498.00
μ (Mo Kα)/cm^{-1}	13.46	13.66	12.17
Independent reflection	4348	8517	4805
Data to parameter ratio	20.04	20.52	23.10
R_1 [$I > 2\sigma(I)$]/No. of Reflection	0.028/3108	0.041/4891	0.037/3905
wR_2 (all data)	0.090/4348	0.128/8517	0.119/4805
GOF	0.99	1.10	1.55

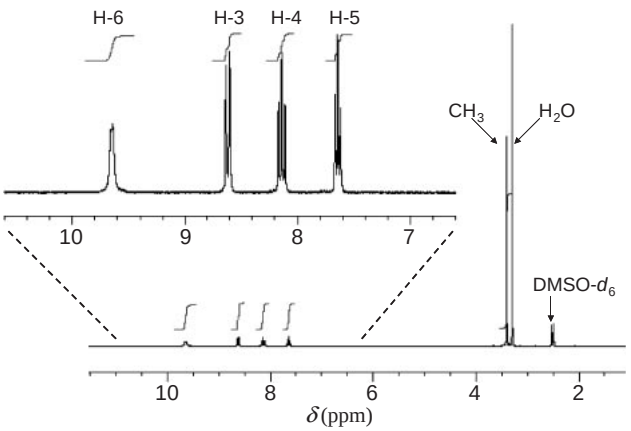

Fig. 1. ^{1}H NMR spectrum of *trans*(Cl),*cis*(S)-[$RuCl_2$(bpy)(dmso-*S*)$_2$] (**1**) in DMSO-d_6.

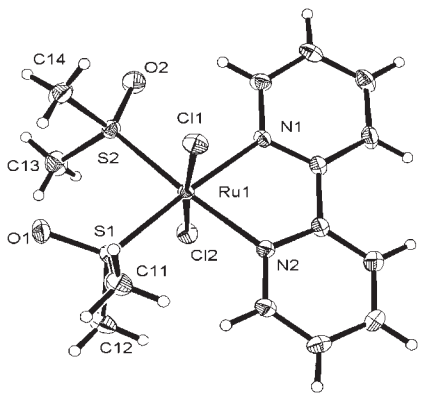

Fig. 2. ORTEP drawing of **1**·H_2O with 30% probability ellipsoids. The H_2O molecule was omitted for clarity.

single crystals that were suitable for X-ray analysis. As shown in the ORTEP drawing in Fig. 2, the Ru ion has a distorted octahedral geometry with two *trans*(Cl) atoms (*trans*(Cl),*cis*(S)-isomer), which is in agreement to the isomer proposed based on the ^{1}H NMR spectrum. Selected bond lengths and angles are listed in Tables 2 and 3, respectively. The Ru(1)–Cl(2) distance (2.400(1) Å) is comparable to that of the starting material, *trans*-[$RuCl_2$(dmso-*S*)$_4$] (2.402(2) Å) and slightly shorter than the Ru(1)–Cl(1) distance (2.416(1) Å). Hydrogen bonding between a H_2O molecule in the unit cell of **1** and the Cl(1) and O(1) atoms explain the small differences between the two Ru–Cl bonds and the two Ru–S bonds. The Ru–S distances (2.273(1) and 2.309(1) Å) were shorter than those of *trans*-[$RuCl_2$(dmso-*S*)$_4$] (2.352(2) Å); the longer Ru–S bond is attributed to competitive π back-bonding between the *trans* dmso ligands and to the steric effects arising from overcrowding within the equatorial plane.[17] The Ru–N distances (2.124(3) and 2.127(3) Å) are significantly longer than those of **2** and **3** and those of previously reported mono(2,2′-bipyridine)ruthenium complexes (2.047–2.083 Å),[11,49,50] which is attributed to the greater *trans* influence of the dmso ligand relative to the other ligands, such as bpy, Cl^-, acetonitrile, and NO^{2-}, and to the steric crowding in the equatorial plane (vide infra).

Significant distortion from the equatorial mean plane, as defined by N(1), N(2), S(1), and S(2), was observed for the four equatorial atoms. The central Ru atom, however, was displaced from the equatorial mean plane toward Cl(1) by only 0.021 Å. The N(1) and S(1) atoms, which are *trans* to each other, were displaced from the mean plane towards Cl(1) by 0.128 and 0.104 Å, respectively. Similarly, N(2) and S(2) were displaced towards Cl(2) by 0.128 and 0.105 Å, respectively. The large distortion suggests significant steric interactions between the bpy and dmso ligands in the *cis*-positions. In addition to the *trans* influence, the *cis* steric effects of the dmso ligands can also cause lengthening of the Ru–N bonds of the bpy ligand. The intramolecular non-bonding contacts of **1** are shown in Fig. 3. The conformation of the two dmso

Table 2. Selected Bond Lengths (Å) for **1**, **2**, and **3**

	trans[a)]	**1**	**2**	**3**
Ru–N bond	Cl		Ru(1)–N(1), 2.080(5)	Ru(1)–N(1), 2.051(3)
			Ru(2)–N(3), 2.065(4)	Ru(1)–N(2), 2.059(3)
	S	Ru(1)–N(1), 2.124(3)	Ru(1)–N(2), 2.083(5)	
		Ru(1)–N(2), 2.127(3)	Ru(2)–N(4), 2.083(5)	
Ru–Cl bond	Cl	Ru(1)–Cl(1), 2.416(1)		
		Ru(1)–Cl(2), 2.400(1)		
	S		Ru(1)–Cl(1), 2.440(2)	
			Ru(2)–Cl(3), 2.438(2)	
	N		Ru(1)–Cl(2), 2.435(2)	Ru(1)–Cl(1), 2.434(1)
			Ru(2)–Cl(4), 2.418(2)	Ru(1)–Cl(2), 2.430(1)
Ru–S bond	Cl		Ru(1)–S(1), 2.244(2)	
			Ru(2)–S(3), 2.232(2)	
	S			Ru(1)–S(1), 2.311(1)
				Ru(1)–S(2), 2.301(1)
	N	Ru(1)–S(1), 2.273(1)	Ru(1)–S(2), 2.281(2)	
		Ru(1)–S(2), 2.309(1)	Ru(2)–S(4), 2.307(2)	

a) Coordinated atom in *trans* position.

Table 3. Selected Bond Angles (deg) for **1**, **2**, and **3**

1	**2**	**3**
Axial		
Cl(1)–Ru(1)–Cl(2), 174.87(3)	Cl(1)–Ru(1)–S(1), 176.34(6)	S(1)–Ru(1)–S(2), 179.52(3)
	Cl(3)–Ru(2)–S(3), 175.37(6)	
Axial–Equatorial		
Cl(1)–Ru(1)–N(1), 85.51(7)	Cl(1)–Ru(1)–N(1), 88.0(1)	S(1)–Ru(1)–N(1), 89.14(8)
Cl(1)–Ru(1)–N(2), 91.97(8)	Cl(1)–Ru(1)–N(2), 83.2(1)	S(1)–Ru(1)–N(2), 89.58(8)
	Cl(3)–Ru(2)–N(3), 86.4(1)	
	Cl(3)–Ru(2)–N(4), 84.1(1)	
Cl(1)–Ru(1)–S(1), 89.35(3)	Cl(1)–Ru(1)–S(2), 93.44(6)	S(1)–Ru(1)–Cl(1), 88.81(3)
Cl(1)–Ru(1)–S(2), 95.01(3)	Cl(1)–Ru(1)–Cl(2), 90.55(6)	S(1)–Ru(1)–Cl(2), 91.11(4)
	Cl(3)–Ru(2)–S(4), 88.07(6)	
	Cl(3)–Ru(2)–Cl(4), 90.86(6)	
Cl(2)–Ru(1)–N(1), 89.89(7)	S(1)–Ru(1)–N(1), 92.5(1)	S(2)–Ru(1)–N(1), 90.41(8)
Cl(2)–Ru(1)–N(2), 84.77(8)	S(1)–Ru(1)–N(2), 93.3(1)	S(2)–Ru(1)–N(2), 90.47(8)
	S(3)–Ru(2)–N(3), 89.0(1)	
	S(3)–Ru(2)–N(4), 94.1(1)	
Cl(2)–Ru(1)–S(1), 95.02(3)	S(1)–Ru(1)–Cl(2), 88.44(6)	S(2)–Ru(1)–Cl(1), 91.66(4)
Cl(2)–Ru(1)–S(2), 87.71(3)	S(1)–Ru(1)–S(2), 90.10(6)	S(2)–Ru(1)–Cl(2), 88.80(3)
	S(3)–Ru(2)–Cl(4), 93.55(6)	
	S(3)–Ru(2)–S(4), 93.58(6)	
Equatorial		
N(1)–Ru(1)–N(2), 77.04(10)	N(1)–Ru(1)–N(2), 78.4(2)	N(1)–Ru(1)–N(2), 79.1(1)
	N(3)–Ru(2)–N(4), 78.4(2)	
S(1)–Ru(1)–S(2), 89.88(3)	Cl(2)–Ru(1)–S(2), 91.48(6)	Cl(1)–Ru(1)–Cl(2), 89.85(4)
	Cl(4)–Ru(2)–S(4), 87.02(6)	
N(1)–Ru(1)–S(2), 95.92(7)	N(1)–Ru(1)–S(2), 96.9(1)	N(1)–Ru(1)–Cl(2), 95.36(8)
	N(3)–Ru(2)–S(4), 100.0(1)	
N(2)–Ru(1)–S(1), 97.80(7)	N(2)–Ru(1)–Cl(2), 93.1(1)	N(2)–Ru(1)–Cl(1), 95.69(8)
	N(4)–Ru(2)–Cl(4), 94.2(1)	

ligands, which can be described as engaged gearwheels, is similar to that of *trans*-[$RuCl_2$(dmso-*S*)$_4$]. The non-bonding contacts between the O(1) atom of dmso-S(1) and the H(17) and H(19) atoms of dmso-S(2) (2.329 and 2.375 Å, respectively) are shorter than the expected H···O distance using van der Waals radii (2.68 Å)[51] but are comparable to the CH···OS distances of Ru^{II} (2.26 and 2.39 Å)[39] and Cd^{II} (2.39(1) Å) complexes.[37] They are also similar to the CH···OC distances in Zn^{II} (2.36–2.53 Å, av. 2.45 Å) and Pt^{II} (2.34(1) Å) complexes.[38] The O(2) atom of the dmso-S(2) points towards the H(4) atom

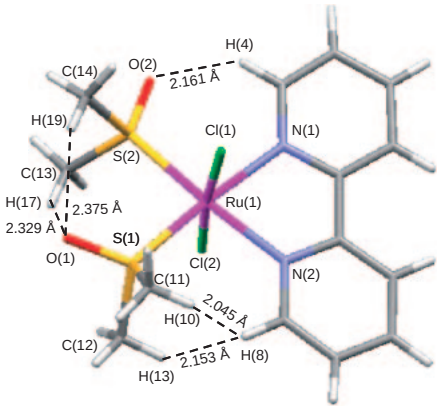

Fig. 3. Intramolecular non-bonding contacts for the crystal structure of **1**.

in the 6-position of the bpy ligand with a torsion angle of 11.8(2)° for O(2)–S(2)–Ru(1)–N(1). Surprisingly, the C–H(4)···O(2) distance (2.161 Å) is significantly shorter than the CH···OS distance for *cis*-[RuCl(bpy)$_2$(dmso-*S*)](PF$_6$) (2.26 Å) which is the shortest distance that has been reported to date.[37–39] Such proximity suggests excessive steric hindrance within the equatorial plane, as defined by the two dmso and bpy ligands, which causes remarkably close contacts and repulsive interactions between O(2) of the dmso-S(2) ligand and H(4) of the proton at the 6-position of the bpy ligand. For the other pyridyl ring of the bpy ligand, the C(11) and C(12) methyl groups of dmso-S(1) squeeze the H(8) atom in the 6′-position of the bpy ligand. The non-bonding distances of 2.045 Å for H(10)···H(8) and 2.153 Å for H(13)···H(8) are somewhat shorter than the expected H···H distance based on the van der Waals radii (2.2 Å).[51] Therefore, the repulsive interactions of 6- and 6′-protons of the bpy ligand towards dmso-S(2) and dmso-S(1), respectively, cause the lengthening of the Ru–N bonds of bpy ligand with significant distortion from the equatorial mean plane. Moreover, the repulsive interactions decrease the thermodynamic stability of **1** in comparison to that of **2**.

The conformations of the two dmso ligands result in the different environments for the four methyl groups. For dmso-S(1), the C(11) and C(12) methyl groups, which are directed towards the bpy ligand, have in similar environments. For dmso-S(2), because the O(2) atom is directed towards bpy ligand, the C(13) and C(14) methyl groups have different environments than that of the methyl groups of dmso-S(1). If the conformations of the dmso ligands in solution are comparable to those in the crystal, at least two methyl signals should be observable in the ^{1}H NMR spectrum. In DMSO solution, however, the four methyl groups of **1** were identical on the ^{1}H NMR time-scale, indicating that the two dmso ligands of **1** should rotate around the Ru–S bonds to give rise to a time-averaged C_{2v} symmetry. The three aromatic upfield signals (δ 7.65, 8.15, and 8.62) were assigned on the basis of their coupling constants.[52] The remaining signal at δ 9.65, which should correspond to the H-6 proton, was observed as a broad singlet (coupling constant cannot be determined). Because the H-6 protons are in close proximity to the dmso ligands on another side of equatorial plane, the broadening of the H-6 proton signal indicates that the bpy ligand is perturbed by the two rotating dmso ligands.

Synthesis and Structure of *cis*(Cl),*cis*(S)-[RuCl$_2$(bpy)-(dmso-*S*)$_2$] (2). When dissolved in DMSO, the thermodynamically unstable **1** slowly isomerizes to **2** along with a small amount of **3**. When dissolved in a solution of EtOH–DMSO (9:1), the isomerization reaction of **1** resulted in the selective precipitation of **2** with high purity and high yields (Method A in synthesis of **2**).

Similarly, although the reaction of *cis*(Cl),*fac*(S)-[RuCl$_2$-(dmso-*S*)$_3$(dmso-*O*)] with bpy in chloroform afforded a mixture of geometrical and linkage isomers, the reaction in EtOH–DMSO (9:1) afforded only **2** in good yield (Method B). The spontaneous precipitation of **2** from the reaction solution allowed for the convenient isolation of the product. As shown in Scheme 1, the preparation of **2** using Method A requires three steps, whereas Method B requires only one step.

The ^{1}H NMR spectrum of **2** in DMSO-d_6 is shown in Fig. 4, and eight aromatic signals with intensities of 1H and four aliphatic singlets with intensities of 3H were observed. The spectral pattern confirms that **2** is an isomer of **1** and that the two pyridine rings of the bpy ligand exist in different environments. Therefore, the Cl$^-$ and dmso ligands occupy *trans*-positions to the bpy ligand (*cis*(Cl),*cis*(S)-isomer).

As shown in Fig. 5, the asymmetric unit of **2** contained two crystallographically independent molecules, Ru(1) and Ru(2). Selected bond lengths and angles are listed in Tables 2 and 3, respectively. Although both Ru ions possess slightly distorted octahedral geometries with the Cl atom *trans* to the S atom of the dmso ligand (*cis*(Cl),*cis*(S)-isomer), the Ru ions had different structural parameters (bond distances and angles) and

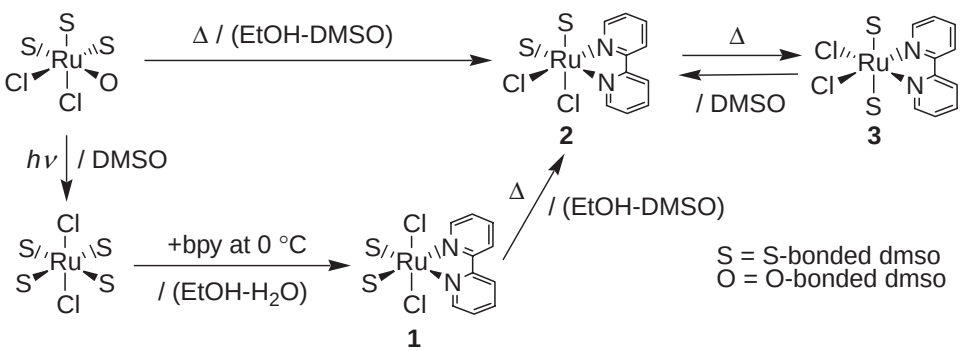

Scheme 1.

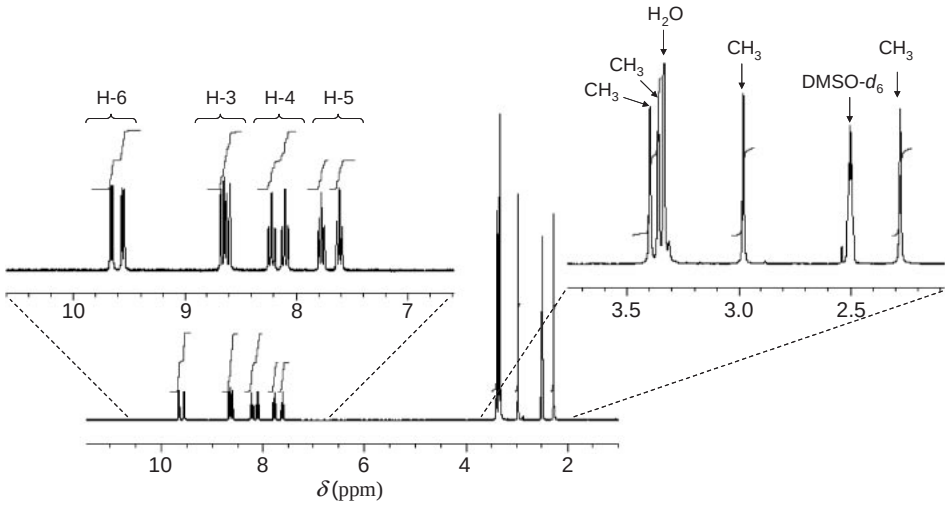

Fig. 4. ^{1}H NMR spectrum of *cis*(Cl),*cis*(S)-[$RuCl_2$(bpy)(dmso-*S*)$_2$] (**2**) in DMSO-d_6.

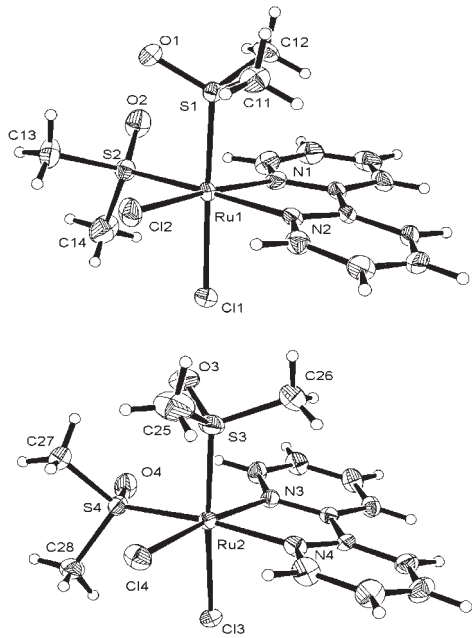

Fig. 5. ORTEP drawing of the two crystallographically independent molecules of **2** with 30% probability ellipsoids.

conformations of the dmso ligands.

The structural parameters around the axial atoms, Cl(1), S(1), Cl(3), and S(3), are comparable for the Ru(1) and Ru(2) molecules. The Ru–Cl distances *trans* to dmso (2.440(2) and 2.438(2) Å) are longer than the corresponding distances (2.416(1) and 2.400(1) Å) for **1** and for *trans*-[$RuCl_2$(dmso-*S*)$_4$] (2.402(2) Å), in which the two Cl atoms are *trans* to each other. This observation is in agreement with the significant influence of the *trans*-dmso ligand. Among **1**, **2**, and **3**, the Ru–S distances *trans* to the Cl atoms (2.244(2) and 2.232(2) Å) are the shortest, and they are comparable to the Ru–S distance that is *trans* to the *O*-bonded dmso in *cis*(Cl),*fac*(S)-[$RuCl_2$(dmso-*S*)$_3$(dmso-*O*)] (2.245(1) Å).[17] This suggests that the axial dmso ligands in **2** are coordinated to Ru without π back-bonding competition and steric influences.

There are, also, some differences in the parameters of the equatorial plane between the two molecules. Ru(1) possesses a relatively undistorted coplanar equatorial mean plane (within $\pm$0.026 Å), as defined by N(1), N(2), Cl(2), and S(2), in which the Ru atom is displaced from this plane towards the dmso-S(1) ligand by 0.038 Å. On the other hand, Ru(2) possesses a distorted equatorial mean plane (0.043–0.055 Å), as defined by N(3), N(4), Cl(4), and S(4), where the Ru atom is displaced towards the dmso-S(3) ligand by 0.099 Å.

The two Ru–N distances (2.080(5) and 2.083(5) Å) for Ru(1) are similar. In the case of Ru(2), however, the Ru(2)–N(3) distance *trans* to Cl(4) (2.065(4) Å) is shorter than the Ru(2)–N(4) distance *trans* to S(4) (2.083(5) Å). This disparity reveals the steric and electronic influences of the dmso ligands within the equatorial planes of dmso-S(2) and dmso-S(4). The Ru(1)–N(2) and Ru(2)–N(4) bonds are *trans* to the dmso ligands, and do not have a dmso ligand *cis* within the equatorial plane—that is, N(2) and N(4) are influenced by *trans*-dmso without steric hindrance from *cis*-dmso within the equatorial plane. Consequently, the Ru(1)–N(2) and Ru(2)–N(4) distances (2.083(5) and 2.083(5) Å, respectively) are shorter than those of **1** (2.124(3) and 2.127(3) Å, respectively), in which the N atoms are subjected to both the influence of *trans*-dmso and the steric hindrance of *cis*-dmso within the equatorial plane.

On the other hand, although Ru(1)–N(1) and Ru(2)–N(3) exist under similar electronic conditions (a Cl atom in the *trans*-position, and without the influence of a *trans*-dmso), their bond distances are different. This different suggests that significant steric interactions occur between the bpy and dmso ligands within the equatorial plane. In the case of Ru(2), the Ru(2)–N(3) distance (2.065(4) Å) is comparable with those of **3** (2.051(3) and 2.059(3) Å), in which the N atoms have *trans*-Cl atoms without any *cis*-dmso within the equatorial plane. In view of the electronic interactions, the Ru(2)–N(3) distance are deemed as reasonable. Steric interactions between the pyridyl-N(3) group and dmso-S(4) cause distortions around the S(4) atom. The Ru(2)–S(4) distance (2.307(2) Å) is longer than the Ru(1)–S(2) distance (2.281(2) Å), and the N(3)–Ru(2)–S(4) angle (100.0(1)°) is greater than the corresponding N(1)–Ru(1)–S(2) angle (96.9(1)°). Steric interactions between the pyridyl-N(1) group and dmso-S(2) result in the elongation

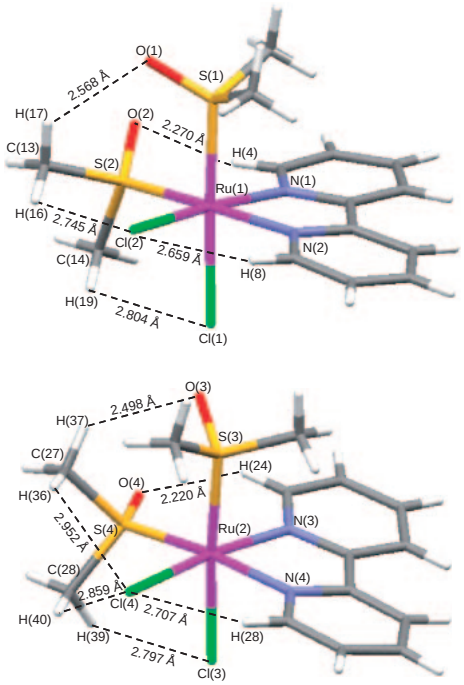

Fig. 6. Intramolecular non-bonding contacts for the crystal structure of **2**.

of the Ru(1)–N(1) bond (2.080(5) Å) in comparison to the Ru(2)–N(3) bond (2.065(4) Å).

From the intramolecular non-bonding contacts in Ru(1) and Ru(2) (Fig. 6), the conformations for the dmso ligands within the equatorial plane of the two molecules are different. For molecule Ru(2), torsion angles of 55.7(3)° for C(27)–S(4)–Ru(2)–Cl(4) and −54.8(3)° for C(28)–S(4)–Ru(2)–Cl(4) indicate that the Cl(4) atom is positioned between the two methyl groups of dmso-S(4). The O(4) atom of dmso-S(4) points towards the H(24) atom in the 6-position of the bpy ligand, and the O(4)–S(4) bond eclipses the Ru(2)–N(3) bond with a torsion angle of −0.4(3)° for O(4)–S(4)–Ru(2)–N(3). The O(4)···H(24) distance (2.220 Å) is comparable to the CH···OS distance in *cis*-[RuCl(bpy)$_2$(dmso-*S*)](PF$_6$) (2.26 Å).[39] For molecule Ru(1), the torsion angles of 17.0(3)° for C(13)–S(2)–Ru(1)–Cl(2) and −96.5(4)° for C(14)–S(2)–Ru(1)–Cl(2) show that the conformation of dmso-S(2) is different than that of dmso-S(4) in Ru(2); dmso-S(2) is twisted from the H(4) atom in the 6-position of the bpy ligand towards dmso-S(1) by ≈40°, with a torsion angle of −39.5(3)° for O(2)–S(2)–Ru(1)–N(1). The O(2)···H(4) distance (2.270 Å) indicates the presence of a hydrogen bond. Furthermore, H(16) of C(13) is adjacent to the Cl(2) ligand with a H(16)···Cl(2) distance of 2.745 Å, which is comparable to the CH···Cl distance in [PtCl$_3$(dmso-S)]$^-$ (2.770 Å).[44] For the C(14) methyl group of dmso-S(2), a CH···Cl interaction was observed for the H(19) atom and the axial Cl(1) atom, and the distance (2.804 Å) is less than the expected H···Cl distance based on the van der Waals radii (2.88 Å).[51] Similarly, another molecule Ru(2) has a CH···Cl hydrogen-bonding interaction between H(39) and Cl(3), with a distance of 2.797 Å. For Ru(1) and Ru(2), the equatorial dmso ligands essentially have similar conformations, in which the sulfoxide O atoms are directed towards the H atoms in the 6-position of the bpy ligand through intramolecular hydrogen bondings (CH···O and CH···Cl). In other words, the conformation of the equatorial dmso ligands are restricted within a narrow space (≈40°).

The conformation of the axial dmso ligand is dependent on that of the equatorial dmso ligand, in which the O atom of the axial dmso ligand is directed towards the methyl group of the equatorial dmso ligand. The closest contact between the two dmso ligands are 2.568 Å (H(17)···O(1)) in molecule Ru(1) and 2.498 Å (H(37)···O(3)) in molecule Ru(2), both of which are shorter than the expected H···O distance based on the van der Waals radii (2.68 Å).[51] It is concluded that these hydrogen bonds play an important role in the conformations of the axial dmso ligands.

In the ^{1}H NMR spectrum of **2** in DMSO-d_6 the four methyl groups of the dmso ligands are not equivalent on the ^{1}H NMR time-scale (δ 2.28, 2.98, 3.37, and 3.40); in other words, the conformations of dmso ligands are restricted, even in a DMSO solution. The intramolecular hydrogen bonds that are observed in the crystal structure should also be evident in a DMSO solution. Through intramolecular hydrogen bonds, the bpy and Cl$^-$ ligands restrict the conformation of equatorial dmso ligand within a narrow space (≈40°). Because the two methyl groups of the equatorial dmso ligand are not equivalent, the restricted equatorial dmso ligand influences the conformation of the axial dmso ligand. As a result, the two methyl groups on the axial dmso ligand exist under dissimilar environments. The chemical shifts of two downfield methyl signals (δ 3.37 and 3.40), which are comparable to that of **1** (δ 3.41), were assigned to the equatorial dmso ligand that is *trans* to the bpy ligand. The remaining two upfield methyl signals (δ 2.28 and 2.98) were assigned to the axial dmso ligand that is *cis* to the bpy ligand due to ring-current effects of the bpy ligand in the *cis*-position. In an attempt to coalesce the four methyl group signals into two signals, variable-temperature ^{1}H NMR experiments were carried out by heating the sample from 30 to 60 °C in DMSO-d_6. However, they were unsuccessful because of rapid exchange of the dmso ligands with the solvent DMSO-d_6.

Furthermore, on another side of the equatorial plane, another non-bonding interaction was observed. The Cl(2)···H(8) and Cl(4)···H(28) distances (2.659 and 2.707 Å, respectively) are significantly shorter than the expected Cl···H distance based on the van der Waals radii (2.88 Å).[51] The monodentate equatorial dmso and Cl$^-$ ligands are involved in hydrogen bonding with the hydrogens in the 6- and 6′-positions of the bpy ligand. The greater thermodynamic stability of **2** over **1** or **3**, which will be described below, is attributed to the hydrogen bonds within the equatorial plane.

Thermal Isomerizations (1 → 2 and 2 ↔ 3). The isomerization reaction of [RuCl$_2$(bpy)(dmso-*S*)$_2$] is summarized in Scheme 1. The reaction rate for the isomerization of **1** to **2** was determined with ^{1}H NMR spectroscopy in DMSO-d_6 at 50 °C. A DMSO-d_6 solution of **1** was sealed in an NMR tube then heated to 50 °C. As the reaction proceeds, the signals of **1** decreased and the signals of **2** increased. After 30 min, in the ^{1}H NMR spectrum of the resulting solution, the signals for **3** appeared, in addition to the signals for **1** and **2**. The decrease in peak intensities of H-6 proton signal of **1**, which were normalized with respect to the sum of intensities of H-6 proton

signals of all species, was plotted over 2 half-lives. It was found to obey simple first-order decay kinetics with a rate constant of $k = (4.0 \pm 0.1) \times 10^{-4}\,s^{-1}$ ($t_{1/2} = 29 \pm 1$ min). This indicates that the reverse reaction to regenerate **1** is very slow compared to the isomerization reaction of **1**, i.e., the isomerization between **1** and **2** is almost irreversible. On the other hand, the increase in peak intensities of **2** did not obey a simple first-order reaction, because of the conversion of **2** to **3**.

A DMSO-d_6 solution of **2** was sealed in an NMR tube then heated to 90 °C. The ^{1}H NMR spectrum of the solution after 1 h of heating is shown in Fig. 7 and had extra signals in addition to the eight signals of **2**. These additional signals at δ 8.50 (2H, d, $J = 8.1$ Hz, H-3) and 9.39 (2H, d, $J = 5.6$ Hz, H-6) were assigned to **3**; the ratio of **2**:**3** is 85/15. The signals for H-4 and H-5 were obscured by the signals of **2**. The remaining small signals, which are labeled with asterisks in Fig. 7b, could not be assigned. Similarly, the isomerization product of **3** as the starting material was consistent with the isomerization product of **2**. Among the three isomers, **2** was found to be the most stable. Although isomerization between **1** and **2** is irreversible, isomerization between **2** and **3** is reversible. Unfortunately, an attempt to determine the reaction rate for the isomerization between **2** and **3** with ^{1}H NMR spectroscopy was unsuccessful because an uncharacterized species, of which the signals were labeled by asterisks in Fig. 7b, appeared in addition to **2** and **3**.

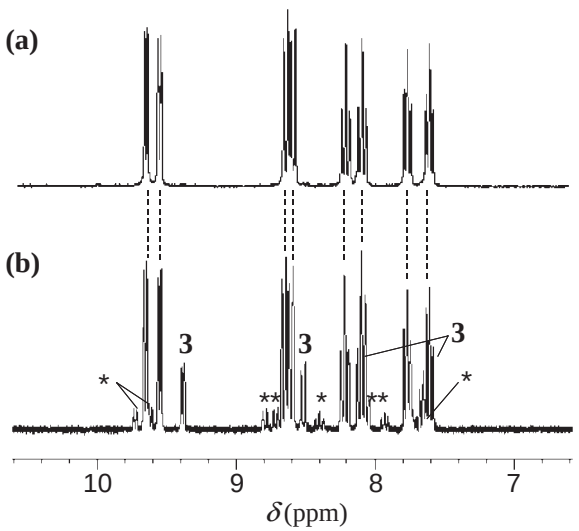

Fig. 7. ^{1}H NMR spectra of **2** in DMSO-d_6: (a) after dissolution, (b) after 1 h heating at 90 °C. ^{1}H NMR spectra were recorded at room temperature (≈25 °C). Signals with asterisks are uncharacterized species.

Structure of *cis*(Cl),*trans*(S)-[RuCl$_2$(bpy)(dmso-*S*)$_2$]·0.5H$_2$O (3·0.5H$_2$O). As described above, **1** and **2** were isolated and characterized by ^{1}H NMR and X-ray crystallography. In contrast, **3** had to be mechanically separated from a mixture of **2** and **3**, which was afforded by the thermal isomerization of **2** in a DMSO solution. Attempts to directly prepare **3** were unsuccessful due to low yields and the facile substitution of the labile dmso ligands. The ^{1}H NMR spectrum of **3** in DMSO-d_6 is shown in Fig. 8 and had four signals with intensities of 2H in the aromatic region and two aliphatic singlets at δ 2.88 and 2.54, which correspond to *S*-bonded and free DMSO, respectively. The sum of intensities of the two aliphatic singlets is 12H. Therefore, the NMR spectrum shows that the dmso ligands in **3** are labile and exchange with the solvent DMSO-d_6. The chemical shift of the methyl protons of **3** (δ 2.88) is upfield compared to that of **1** (δ 3.41), in which the dmso ligands are *trans* to the bpy ligand. Presumably, the dmso ligands of **3** are *cis* to the bpy ligand, i.e., *cis*(Cl),-*trans*(S)-isomer, and are influenced by its ring-current effects.

The crystal structure of **3** is shown in Fig. 9, and selected bond lengths and angles are listed in Tables 2 and 3, respec-

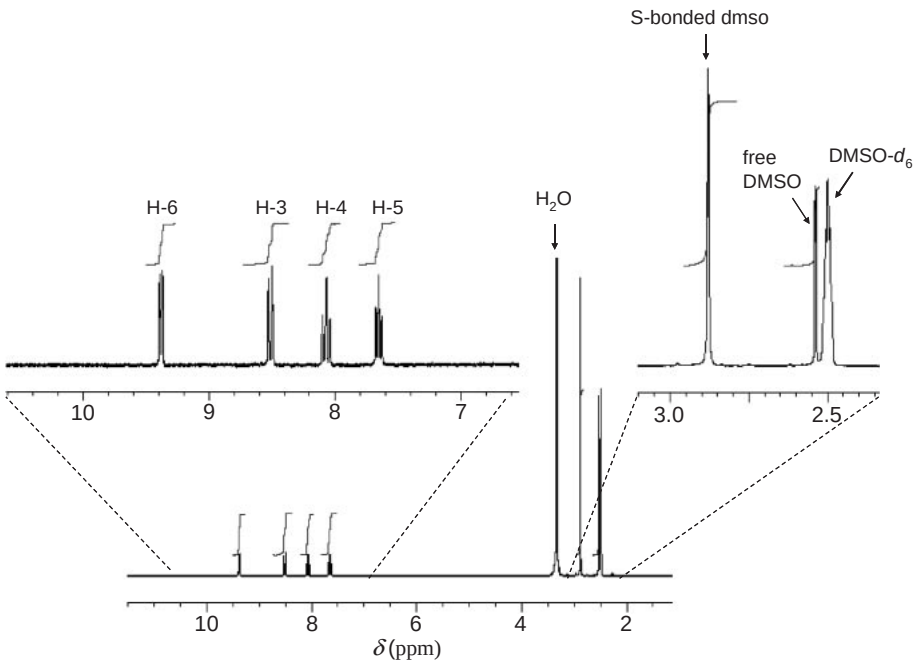

Fig. 8. ^{1}H NMR spectrum of *cis*(Cl),*trans*(S)-[RuCl$_2$(bpy)(dmso-*S*)$_2$] (**3**) in DMSO-d_6.

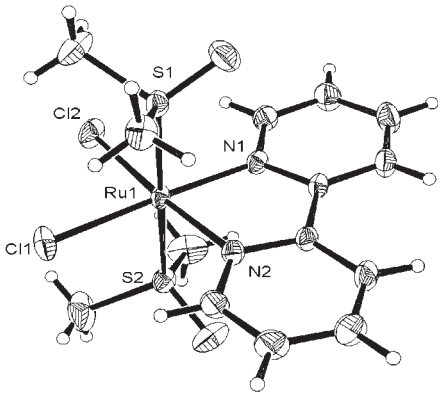

Fig. 9. ORTEP drawing of $3 \cdot 0.5H_2O$ with 30% probability ellipsoids. The H_2O molecule was omitted for clarity.

tively. The Ru ion of **3** has an octahedral geometry with two *trans* or axial S atoms (*cis*(Cl),*trans*(S)-isomer). The four equatorial atoms, N(1), N(2), Cl(1), and Cl(2), are coplanar to within ±0.029 Å, and the Ru ion is displaced from this plane by 0.013 Å. The angles formed by the axial S atoms and the equatorial atoms range from 91.66(4) to 88.80(3)°. The geometry around the Ru ion is somewhat typical, with the exception of the chelate bite angle (79.1(1)°) for the bpy ligand. The Ru–N distances (2.051(3) and 2.059(3) Å), which are *trans* to a Cl atom, are shorter than those of **1** and **2**. The Ru–Cl distances (2.434(1) and 2.430(1) Å) are comparable to those that are *trans* to the N atom in **2** (2.435(2) and 2.418(2) Å). The Ru–S distances (2.311(1) and 2.301(1) Å), which are *trans* to each other, are shorter than those in *trans*-[$RuCl_2$(dmso-*S*)$_4$] (2.352(2) Å). Since the electronic π-interactions of the dmso ligands in **3** are similar to those of *trans*-[$RuCl_2$(dmso-*S*)$_4$], the lengthening of the Ru–S bonds in the latter is attributable to the steric influence by *cis*-dmso. The Cl(1)···H(8) and Cl(2)···H(4) distances (2.737 and 2.723 Å, respectively) indicate that the Cl^- ligands interact with bpy ligand through hydrogen bonds. Although these structural features suggest a higher stability, **3** is actually less stable and more prone to isomerization than **2** in a DMSO solution. The lower stability of **3** can be explained by competitive π back-bonding between the *trans* dmso ligands.

Conclusion

The selective synthesis and characterization using X-ray analysis of the *trans*(Cl),*cis*(S)- and *cis*(Cl),*cis*(S)-isomers of [$RuCl_2$(bpy)(dmso-*S*)$_2$] (**1** and **2**, respectively) were accomplished. Although the *cis*(Cl),*trans*(S)-isomer (**3**) was not independently isolated, its geometry was also verified using X-ray crystallography. The three compounds underwent isomerization in a DMSO solution. In contrast to the reversible isomerization between **2** and **3**, isomerization from **1** to **2** is irreversible.

Our results show that intramolecular non-bonding interactions between the bpy and dmso ligands within the equatorial plane explain the distortion, stability, and spectral features of **1** and **2**. In the crystal structure of **1**, the 6- and 6′-protons of the bpy ligand repulse the two dmso ligands within the equatorial plane. The undesirable steric interactions decrease the thermodynamic stability of **1** in comparison to those of **2** and **3**. The rotation of the dmso ligands in close proximity to the H-6 protons of bpy ligand causes broadening of the H-6 ^{1}H NMR signal. In the crystal structure of **2**, the bpy ligand directly controls the conformation of the equatorial dmso ligand through a CH···O hydrogen bond, while indirectly controlling that of the axial dmso ligand. The ^{1}H NMR spectrum of **2** in DMSO-d_6 indicates that the rotation of the two dmso ligands are restricted by hydrogen bonding, even in a DMSO solution.

Experiments are currently underway to explore the applicability of our synthesis of mono(polypyridyl)ruthenium complexes to other polypyridyl ligands.

This work was financially supported by Research Project Grant (B) by Institute of Science and Technology, Meiji University.

References

1 A. Juris, V. Balzani, F. Barigelletti, S. Campagna, P. Belser, A. von Zelewsky, *Coord. Chem. Rev.* **1988**, *84*, 85.
2 V. Balzani, A. Juris, M. Venturi, S. Campagna, S. Serroni, *Chem. Rev.* **1996**, *96*, 759.
3 F. Barigelletti, L. Flamigni, *Chem. Soc. Rev.* **2000**, *29*, 1.
4 T. J. Meyer, *Pure Appl. Chem.* **1986**, *58*, 1193.
5 I. P. Evans, A. Spencer, G. Wilkinson, *J. Chem. Soc., Dalton Trans.* **1973**, 204.
6 S. M. Zakeeruddin, M. K. Nazeeruddin, R. Humphry-Baker, M. Grätzel, V. Shklover, *Inorg. Chem.* **1998**, *37*, 5251.
7 T. Suzuki, T. Kuchiyama, S. Kishi, S. Kaizaki, H. D. Takagi, M. Kato, *Inorg. Chem.* **2003**, *42*, 785.
8 D. A. Freedman, J. K. Evju, M. K. Promije, K. R. Mann, *Inorg. Chem.* **2001**, *40*, 5711.
9 G. F. Srouse, P. A. Anderson, J. R. Schoonover, T. J. Meyer, F. R. Keene, *Inorg. Chem.* **1992**, *31*, 3004.
10 P. A. Anderson, G. B. Deacon, K. H. Haarman, F. R. Keene, T. J. Meyer, D. A. Reitsma, B. W. Skelton, G. F. Strouse, N. C. Thomas, J. A. Treadway, A. H. White, *Inorg. Chem.* **1995**, *34*, 6145.
11 D. Hesek, Y. Inoue, S. R. L. Everitt, H. Ishida, M. Kunieda, M. G. B. Drew, *Inorg. Chem.* **2000**, *39*, 308.
12 A. von Zelewsky, G. Gremaud, *Helv. Chim. Acta* **1988**, *71*, 1108.
13 R. P. Thummel, F. Lefoulon, S. Chirayil, *Inorg. Chem.* **1987**, *26*, 3072.
14 L. Spiccia, G. B. Deacon, C. M. Kepert, *Coord. Chem. Rev.* **2004**, *248*, 1329.
15 M. B. Cingi, M. Lanfranchi, M. A. Pellinghelli, M. Tegoni, *Eur. J. Inorg. Chem.* **2000**, 703.
16 C. Sens, M. Rodriguez, I. Romero, A. Llobet, *Inorg. Chem.* **2003**, *42*, 2040.
17 E. Alessio, G. Mestroni, G. Nardin, W. M. Attia, M. Calligaris, G. Sava, S. Zorzet, *Inorg. Chem.* **1988**, *27*, 4099.
18 G. Mestroni, E. Alessio, M. Calligaris, W. M. Attia, F. Quadrifoglio, S. Cauci, G. Sava, S. Zorzet, S. Pacor, C. Monti-Bragadin, M. Tamaro, L. Dolzani, *Prog. Clin. Biochem. Med.* **1989**, *10*, 71.
19 G. Sara, S. Pacor, S. Zorzet, E. Alessio, G. Mestroni, *Pharmacol. Res.* **1989**, *21*, 617.
20 C. B. Aakeröy, K. R. Seddon, *Chem. Soc. Rev.* **1993**, *22*, 397.
21 G. R. Desiraju, *Angew. Chem., Int. Ed. Engl.* **1955**, *34*, 2311.

22 M. D. Ward, F. Barigelletti, *Coord. Chem. Rev.* **2001**, *216–217*, 127.
23 S. Kitagawa, S. Kawata, *Coord. Chem. Rev.* **2002**, *224*, 11.
24 S. Tsuzuki, H. Houjou, Y. Nagawa, K. Hiratani, *J. Chem. Soc., Perkin Trans. 2* **2001**, 1951.
25 S. Tsuzuki, H. Houjou, Y. Nagawa, K. Hiratani, *J. Chem. Soc., Perkin Trans. 2* **2002**, 1271.
26 J. Chocholoušová, V. Špirko, P. Hobza, *Phys. Chem. Chem. Phys.* **2004**, *6*, 37.
27 Y. Gu, T. Kar, S. Scheiner, *J. Am. Chem. Soc.* **1999**, *121*, 9411.
28 G. R. Desiraju, *Acc. Chem. Res.* **1991**, *24*, 290.
29 R. Taylor, O. Kennard, *J. Am. Chem. Soc.* **1982**, *104*, 5063.
30 P. W. Baures, A. M. Beatty, M. Dhanasekaran, B. A. Helfrich, W. Pérez-Segarra, J. Desper, *J. Am. Chem. Soc.* **2002**, *124*, 11315.
31 T. Steiner, W. Saenger, *J. Am. Chem. Soc.* **1993**, *115*, 4540.
32 P. W. Baures, A. Wiznycia, A. M. Beatty, *Bioorg. Med. Chem.* **2000**, *8*, 1599.
33 Y. Mandel-Gutfreund, H. Margalit, R. L. Jernigan, V. B. Zhurkin, *J. Mol. Biol.* **1998**, *277*, 1129.
34 Z. S. Derewenda, L. Lee, U. Derewenda, *J. Mol. Biol.* **1995**, *252*, 248.
35 S. Defazio, R. Cini, *J. Chem. Soc., Dalton Trans.* **2002**, 1888.
36 D. L. Reger, J. R. Gardinier, M. D. Smith, *Inorg. Chim. Acta* **2003**, *352*, 151.
37 S. Defazio, R. Cini, *Polyhedron* **2003**, *22*, 1355.
38 B. Jasiewicz, W. Boczoń, B. Warżajtis, U. Rychlewskal, T. Rafałowicz, *J. Mol. Struct.* **2005**, *753*, 45.
39 D. Hesek, Y. Inoue, S. R. L. Everitt, H. Ishida, M. Kunieda, M. G. B. Drew, *J. Chem. Soc., Dalton Trans.* **1999**, 3701.
40 D. Hesek, Y. Inoue, S. R. L. Everitt, H. Ishida, M. Kunieda, M. G. B. Drew, *Inorg. Chem.* **2000**, *39*, 317.
41 M. Freytag, P. G. Jones, *Chem. Commun.* **2000**, 277.
42 K. R. Flower, L. G. Leal, R. G. Pritchard, *J. Organomet. Chem.* **2005**, *690*, 3390.
43 V. Chandrasekhar, V. Baskar, S. Kingsley, S. Nagendran, R. J. Butcher, *CrystEngComm* **2001**, *17*, 1.
44 R. Cini, A. Donati, R. Giannettoni, *Inorg. Chim. Acta* **2001**, *315*, 73.
45 R. Cini, A. Cavaglioni, *Inorg. Chem.* **1999**, *38*, 3751.
46 T. Spaniel, H. Görls, J. Scholz, *Angew. Chem., Int. Ed.* **1998**, *37*, 1862.
47 L.-Y. Huang, U. R. Aulwurm, F. W. Heinemann, F. Knoch, H. Kisch, *Chem. Eur. J.* **1998**, *4*, 1641.
48 *teXsan Crystal Structure Analysis Package*, Molecular Structure Corporation, **1992**.
49 D. A. Freedman, D. E. Janzen, J. L. Vreeland, H. M. Tully, K. R. Mann, *Inorg. Chem.* **2002**, *41*, 3820.
50 M. Haukka, T. Venäläinen, M. Ahlgrén, T. A. Pakkanen, *Inorg. Chem.* **1995**, *34*, 2931.
51 R. S. Rowland, R. Taylor, *J. Phys. Chem.* **1996**, *100*, 7384.
52 N. Nagao, M. Mukaida, S. Tachiyashiki, K. Mizumachi, *Bull. Chem. Soc. Jpn.* **1994**, *67*, 1802.